Molecular dynamics study on condensation/evaporation coefficients of chain molecules at liquid–vapor interface

Gyoko Nagayama, Masaki Takematsu, Hirotaka Mizuguchi, and Takaharu Tsuruta

Citation: The Journal of Chemical Physics **143**, 014706 (2015); doi: 10.1063/1.4923261
View online: http://dx.doi.org/10.1063/1.4923261
View Table of Contents: http://scitation.aip.org/content/aip/journal/jcp/143/1?ver=pdfcov
Published by the AIP Publishing

Molecular dynamics study on condensation/evaporation coefficients of chain molecules at liquid–vapor interface

Gyoko Nagayama,[a] Masaki Takematsu, Hirotaka Mizuguchi, and Takaharu Tsuruta
Department of Mechanical Engineering, Kyushu Institute of Technology, Kitakyushu, Fukuoka 804-8550, Japan

(Received 14 May 2015; accepted 18 June 2015; published online 7 July 2015)

The structure and thermodynamic properties of the liquid–vapor interface are of fundamental interest for numerous technological implications. For simple molecules, e.g., argon and water, the molecular condensation/evaporation behavior depends strongly on their translational motion and the system temperature. Existing molecular dynamics (MD) results are consistent with the theoretical predictions based on the assumption that the liquid and vapor states in the vicinity of the liquid–vapor interface are isotropic. Additionally, similar molecular condensation/evaporation characteristics have been found for long-chain molecules, e.g., dodecane. It is unclear, however, whether the isotropic assumption is valid and whether the molecular orientation or the chain length of the molecules affects the condensation/evaporation behavior at the liquid–vapor interface. In this study, MD simulations were performed to study the molecular condensation/evaporation behavior of the straight-chain alkanes, i.e., butane, octane, and dodecane, at the liquid–vapor interface, and the effects of the molecular orientation and chain length were investigated in equilibrium systems. The results showed that the condensation/evaporation behavior of chain molecules primarily depends on the molecular translational energy and the surface temperature and is independent of the molecular chain length. Furthermore, the orientation at the liquid–vapor interface was disordered when the surface temperature was sufficiently higher than the triple point and had no significant effect on the molecular condensation/evaporation behavior. The validity of the isotropic assumption was confirmed, and we conclude that the condensation/evaporation coefficients can be predicted by the liquid-to-vapor translational length ratio, even for chain molecules. [http://dx.doi.org/10.1063/1.4923261]

I. INTRODUCTION

Phase-change phenomena at the liquid–vapor interface are of fundamental and current interest for advanced engineering applications, such as spray combustion, spray cooling, and droplet evaporation in super-fine inkjet printing. The condensation/evaporation coefficients are important parameters in determining the mass and heat transfer rate at the liquid–vapor interface. However, such parameters are difficult to investigate experimentally, and most of the available data are limited to those parameters obtained from macroscopic information. Despite decades of study, uncertainty regarding the condensation and evaporation rates at the liquid–vapor interface of simple or complex components remains,[1–4] and the condensation/evaporation coefficients are often determined empirically.

The liquid–vapor interface is typically a couple of molecular diameters thick; hence, molecular dynamics (MD) simulations are an effective tool for examining the mechanisms of liquid–vapor phase change. A considerable number of studies have been devoted to the liquid–vapor interface using MD simulations, and much attention has been given to the determination of the condensation/evaporation coefficient.[5–33] Conventionally, the condensation/evaporation coefficient is defined as the ratio of the mass flux condensing onto/evaporating from a liquid surface to the maximum flux determined by the kinetic theory of gases. Microscopic reversibility requires that the condensing flux and the evaporating flux for an equilibrium system are equivalent. Hence, the condensation coefficient is equal to the evaporation coefficient at the equilibrium liquid–vapor interface. The above definition, based on the kinetic theory of gases, is usually represented in MD as

$$\overline{\sigma}_c = N_c/N_{in} \text{ or } \overline{\sigma}_e = N_e/N_{out}. \quad (1)$$

Here, $\overline{\sigma}_c$ is the macroscopic condensation coefficient, N_c is the condensed molecular number, N_{in} is the incoming molecular number, $\overline{\sigma}_e$ is the macroscopic evaporation coefficient, N_e is the evaporated molecular number, and N_{out} is the outgoing molecular number. Another definition is related to the condensation/evaporation probability of each molecule corresponding to its initial translational energy level,[16]

$$\sigma_c = N_c(E_z)/N_{in}(E_z) \text{ or } \sigma_e = N_e(E_z)/N_{out}(E_z), \quad (2)$$

where E_z is the normal component of the molecular translational energy. For a clearer distinction, σ_c is hereafter called the microscopic condensation coefficient and σ_e is the microscopic evaporation coefficient. Obviously, $\overline{\sigma}_c$ and $\overline{\sigma}_e$ are the mean values of σ_c and σ_e, respectively.

In most of the existing literature, the macroscopic condensation/evaporation coefficient is considered to have a uniform value irrespective of the kinetic motion of the molecules. A condensation/evaporation coefficient of unity means a zero energetic barrier; i.e., all molecules approaching the interface

[a]Author to whom correspondence should be addressed. Electronic mail: nagayama@mech.kyutech.ac.jp

completely condense into the liquid phase without reflection and those departing from the interface completely evaporate to the vapor phase. On the other hand, condensation/evaporation coefficients smaller than unity imply a kinetic barrier to the condensation/evaporation process.[14,15] Hence, the condensing or evaporating molecules must pass through a transition state involving an energetic barrier when the molecules migrate through the liquid–vapor interface during the phase change. As shown in Fig. 1, the mechanism of the energetic barrier has been attributed to the restricted translational motion of molecules (i.e., the free volume restriction). A simple theoretical expression of the macroscopic condensation/evaporation coefficient has been derived by Nagayama and Tsuruta based on the transition state theory and MD simulations,[15]

$$\overline{\sigma}_e = \overline{\sigma}_c = \left(1 - \sqrt[3]{v_l/v_g}\right) \exp\left(-\frac{1}{2}\frac{1}{\sqrt[3]{v_g/v_l} - 1}\right), \quad (3)$$

where v_l and v_g are the free volumes of the liquid and vapor molecules, respectively. The cubic root of the free volumes concerns the assumption of the isotropic phase of liquid and vapor in the vicinity of the liquid–vapor interface (Fig. 1(a)),

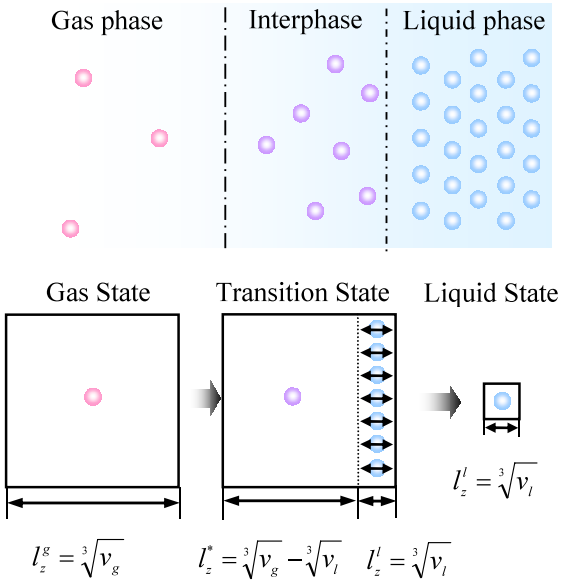

(a) The isotropic model of free volume restriction in the transition state at the liquid–vapor interface for simple molecules. [15]

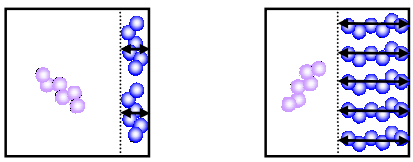

(b) Possible anisotropic cases of free volume restriction in the transition state for chain molecules: parallel orientation (left) and perpendicular orientation (right).

FIG. 1. The theoretical model of free volume restriction in the transition state at the liquid–vapor interface. (a) The isotropic model of free volume restriction in the transition state at the liquid–vapor interface for simple molecules.[15] (b) Possible anisotropic cases of free volume restriction in the transition state for chain molecules: parallel orientation (left) and perpendicular orientation (right).

i.e., the molecular structure or shape is irrelevant to the condensation/evaporation coefficient. Equation (3) is valid for molecules to which the isotropic assumption can be applied. However, as shown in Fig. 1(b), this assumption might be invalid if the orientation of the molecule's long chain is parallel or perpendicular to the liquid–vapor interface.

TABLE I. MD simulation results of the macroscopic condensation/evaporation coefficients.

Substance	Authors/method	Temperature, K	$\bar{\sigma}_c$ or $\bar{\sigma}_e$
Argon or Lennard-Jones fluids	Yasuoka *et al.*[6]/ equilibrium planar interface	80	0.80
		100	0.80
	Matsumoto[10]/ equilibrium planar interface	110	0.40
		120	0.15
		130	0.05
	Tsuruta *et al.*[16] and Nagayama and Tsuruta[15]/ equilibrium planar interface	84	0.93
		90	0.83
		102	0.79
		120	0.61
		130	0.50
	Gu *et al.*[19]/ equilibrium planar liquid-vapor interface upon solid wall	90	0.69
		100	0.66
		110	0.59
		120	0.44
		130	0.28
Water	Yasuoka *et al.*[8]	400	0.40
		350	0.35
	Matsumoto[10]/ equilibrium planar interface	400	0.30
		450	0.15
		500	0.05
	Nagayama and Tsuruta[14]/ equilibrium planar interface	330	0.96
		450	0.83
		474	0.80
		500	0.55
		515	0.49
		550	0.29
Methanol	Matsumoto *et al.*[7]/ equilibrium planar interface	300	0.20
		350	0.25
Dodecane	Xie *et al.*[20] and Cao *et al.*[21]/ equilibrium planar interface	400	0.93
		450	0.72
		500	0.59
		550	0.45
		600	0.30
	Mizuguchi *et al.*[23]/ equilibrium planar interface	300	0.99
		350	0.99
		400	0.97
		450	0.93
		500	0.81
		550	0.64
Butane	Nagayama *et al.*[24]/ equilibrium planar interface	270	0.84
		300	0.74
		320	0.63
		340	0.52
Octane	Nagayama *et al.*[24]/ equilibrium planar interface	400	0.82
		430	0.75
		450	0.68
		460	0.63

Table I lists the macroscopic condensation/evaporation coefficient data obtained by MD simulations at different temperatures for various liquid–vapor interfaces at equilibrium. Most of the results were obtained at surface temperatures between the triple point and critical point, where the liquid–vapor phase-change phenomena can be simulated. Despite the different simulation methods and simulated substances, one of the most common conclusions obtained in previous publications is that the condensation/evaporation coefficient is surface-temperature dependent. As shown in Table I, the macroscopic condensation/evaporation coefficient decreases with increasing surface temperature, i.e., the results are close to unity at the triple point and decrease to zero at the critical point. Since the density, i.e., the specific volume of liquid or vapor, is a function of temperature, Eq. (3) establishes the dependence of the theoretical condensation/evaporation coefficients on temperature, allowing a comparison of the theory and the MD results. As shown in Fig. 2, the MD simulation results for argon,[16,19,28,32,33] water,[14,29] and dodecane[20,21,24] are in agreement with Eq. (3). Contrary to our expectations, the molecular structure and the chain length have no significant effect on the condensation/evaporation coefficient. It is not clear, however, why the chain molecule (dodecane) has a condensation/evaporation behavior similar to molecules like argon or water and whether Eq. (3) is valid for chain molecules. Therefore, in this study, MD simulations were performed to study the molecular condensation/evaporation behavior as well as the liquid–vapor interface structure of a group of carbon chain molecules: butane (C_4H_{10}), octane (C_8H_{18}), and dodecane ($C_{12}H_{26}$). The effects of the molecular orientation and chain length on the molecular condensation/evaporation behavior in equilibrium systems were investigated.

II. METHODOLOGY

For the MD simulations, three carbon chain molecules with different chain lengths were examined: butane CH_3-$(CH_2)_2$-(CH_3), octane CH_3-$(CH_2)_6$-(CH_3), and dodecane CH_3-$(CH_2)_{10}$-(CH_3); their molecular structures and volume images are shown in Fig. 3. The chain length and diameter of the cylindrical volume are obtained from a single molecule structure based on the Gaussian 09 model.[34] The particle numbers and sizes of the simulation cells are listed in Table II. The temperature of the simulation system ranged between the triple and critical points. The basic cell was a rectangular box with dimensions of $L_x \times L_y \times L_z$ (see Table II), and a thin liquid film consisting of liquid molecules was formed at the central region, as shown in Fig. 3.

The MD simulations were performed using AMBER versions 10 and 12.[35] The general Amber force field (GAFF) was applied, and the particle mesh Ewald method was used to efficiently compute long-range electrostatic force terms. The potential energy E_{tot} is the sum of the following terms:

$$E_{tot} = \sum_{bonds} K_r(r - r_{eq})^2 + \sum_{angles} K_\theta(\theta - \theta_{eq})^2 + \sum_{torsions} \frac{V_n}{2}[1 + \cos(n\phi - \gamma)] + \sum_{i<j}^{atoms} \left(\frac{A_{ij}}{R_{ij}^{12}} - \frac{B_{ij}}{R_{ij}^{6}}\right) + \sum_{i<j}^{atoms} \frac{q_i q_j}{\varepsilon R_{ij}}, \quad (4)$$

where K_r, r_{eq}, K_θ, θ_{eq}, V_n, n, γ, A_{ij}, B_{ij}, q_i, q_j, and ε are parameters to be specified in the parameter files for GAFF.[36] The first term in Eq. (4) describes the bond stretching, where K_r is the force constant and r_{eq} is the equilibrium bond length. The second term represents the angle bending term, which is parameterized by force constant K_θ and equilibrium angle θ_{eq}. The third term is the usual Fourier-series expansion for torsional terms, including the torsion barrier V_n, periodicity n, and phase γ. The torsion term is divided into individual contributions for each pair of atoms involved in the torsion. The fifth term is the van der Waals interaction between nonbonded atoms i and j, where R_{ij} is the distance between the two atoms and A_{ij} and B_{ij} are specific parameters for atomic pairs i and j. The last term describes the Coulomb interaction for partial charges.

All simulations were performed in the canonical ensemble (NVT) of quasi-equilibrium systems with a time step of 0.5 fs, a cutoff radius of 15 Å, and periodic boundary conditions in all directions. After achieving a steady state from the initial state, the equilibrium system was simulated without a thermostat. Then, the data were sampled under steady equilibrium

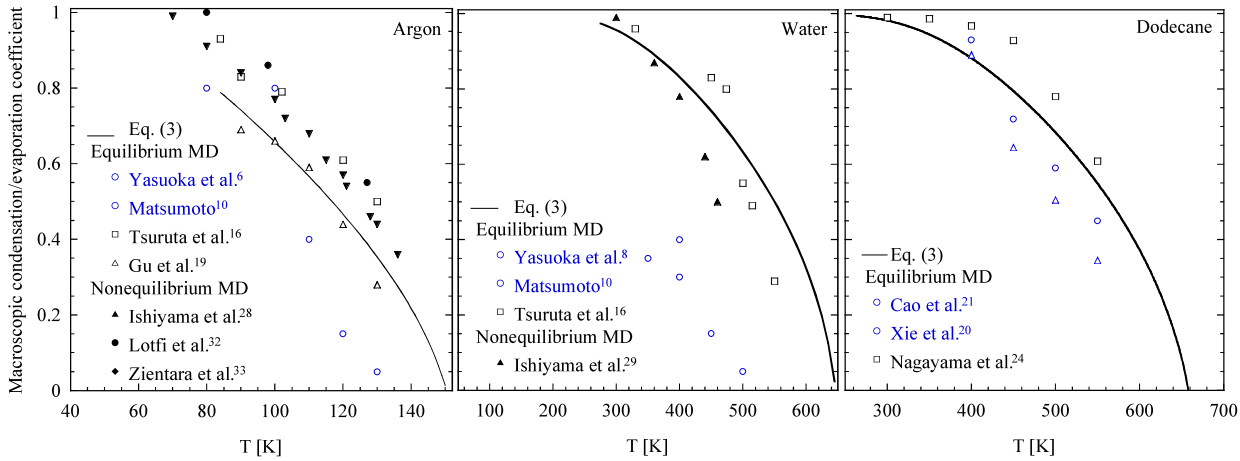

FIG. 2. Macroscopic condensation/evaporation coefficients as a function of temperature.

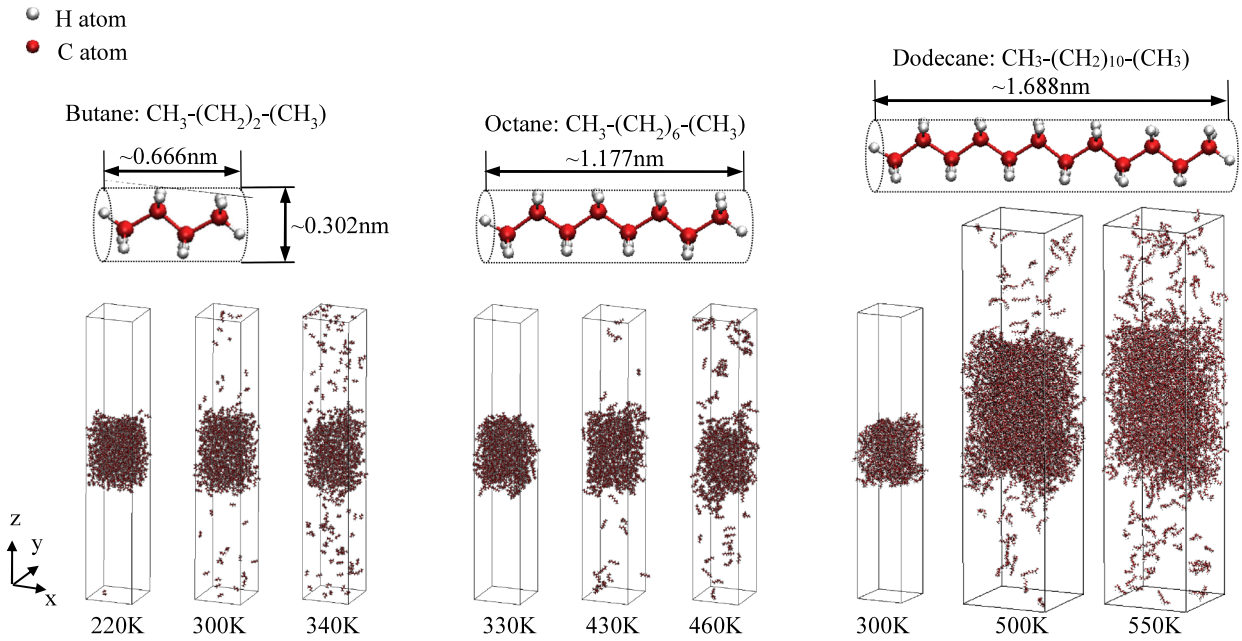

FIG. 3. Molecular structures of the examined carbon chain molecules and sample snapshots of the simulation systems in the equilibrium state at different temperatures.

conditions for approximately 5 ns. The details of data sampling are described elsewhere.[14,16,24] Figure 3 shows snapshots of the simulated systems in the equilibrium state for butane, octane, and dodecane at different temperatures.

III. RESULTS AND DISCUSSION

A. Density profiles

Figure 4 shows the density profiles of all simulation cells in equilibrium. The results of the bulk liquid and the bulk vapor agree well with those in previous studies.[37] The density profiles for butane, octane, and dodecane (except at 300 K) have the typical shape of the liquid–vapor interface. However, it should be noted that the two liquid density peaks for dodecane at 300 K (Fig. 4(c)) show higher density at the interface than in the bulk liquid. This implies that the long-chain molecules at the interface tend to be highly oriented with decreasing temperature, while the chain length has less effect on the interface density when the temperature is sufficiently high.

B. Microscopic condensation/evaporation coefficient

Figure 5 shows the results for the microscopic condensation/evaporation coefficients of the liquid film at different temperatures for butane, octane, and dodecane. The molecule with the larger translational energy normal to the liquid surface condenses/evaporates more easily than that with the lower translational energy. Furthermore, the microscopic condensation/evaporation coefficient decreases when the temperature of the liquid film increases. This implies that the condensation/evaporation behavior of the examined long-chain molecules is similar to that of simple particles, such as argon and water. Hence, the molecular chain length does not significantly affect the liquid–vapor phase-change phenomena. As a result, the condensation/evaporation coefficient of chain molecules can be expressed in the same form as that proposed in previous studies,[16]

$$\sigma_c = \sigma_e = \left\{1 - \beta \exp\left(-\frac{mV_z^2}{2k_BT}\right)\right\} \times \alpha, \tag{5}$$

TABLE II. Simulation systems and parameters.

	Butane	Octane	Dodecane	
Molecular weight	58.12	114.23	170.33	
Chain length (nm)	0.487	0.995	1.496	
Triple point (K)	134.60	216.20	263.16	
Critical point, T_c (K)	425.10	569.30	658.10	
Specific volume at critical point per mole, v_c (nm^3/mole)	0.423	0.808	1.249	
Molecular volume, $v_m(=v_c/3)$ (nm^3/mole)	0.141	0.269	0.416	
Temperature (K)	220–340	330–460	300–450	500–550
Molecules (atoms)	560 (7840)	294 (7644)	208 (7904)	1020 (38 760)
L_x (nm)×L_y (nm)×L_z (nm)	4×4×24	4×4×24	4×4×24	7×7×30

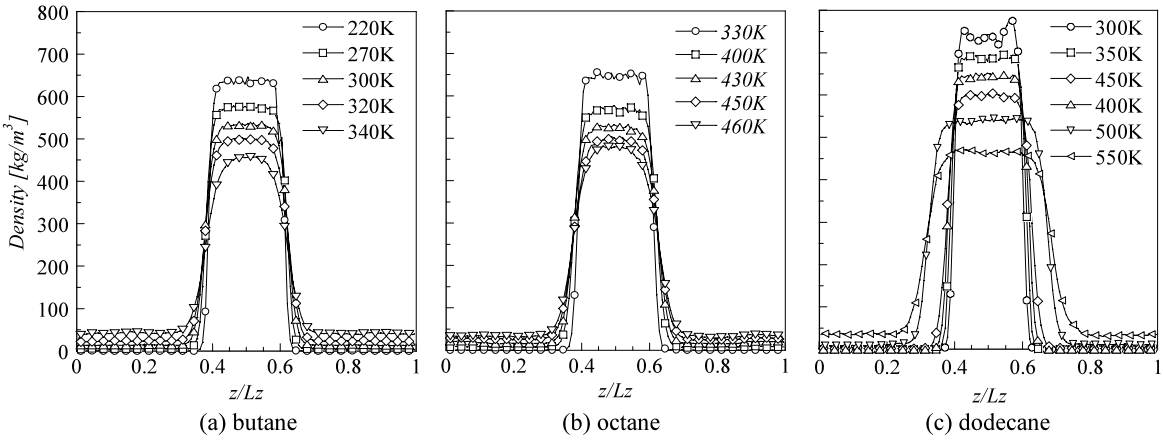

FIG. 4. Density profiles of (a) butane, (b) octane, and (c) dodecane in equilibrium systems.

where m is the molecular weight, V_z is the velocity normal to the liquid–vapor interface, k_B is the Boltzmann constant, T is the liquid temperature, and α and β are the fitting parameters related to the translational length ratio.[15] The MD simulation results for parameters α and β at different temperatures are summarized in Table III.

C. Macroscopic condensation/evaporation coefficient

Under thermal equilibrium conditions, the number flux of the incident molecules can be given by a Maxwellian velocity distribution. Thus, the mean value of the microscopic condensation/evaporation coefficient, i.e., the macroscopic condensation/evaporation coefficient, is obtained by calculating the integral of Eq. (5) in the half range of a Maxwellian ensemble,

$$\overline{\sigma}_c = \overline{\sigma}_e = \frac{1}{(k_BT/2\pi m)^{1/2}} \int_0^\infty \sigma_c V_z \left(\frac{m}{2\pi k_BT}\right)^{1/2} \times \exp\left(-\frac{mV_z^2}{2k_BT}\right) dV_z = \alpha\left(1 - \beta/2\right) \quad (6)$$

The physical meaning of parameters α and β can be clarified by the connection between Eq. (6) and the transition state theory as

$$\alpha = \exp\left(-\frac{1}{2}\frac{1}{\sqrt[3]{\nu_g/\nu_l} - 1}\right) \text{ and } \beta = 2\sqrt[3]{\nu_l/\nu_g}. \quad (7)$$

Here, α relates to the activation energy and β implies the translational energy dependence of the microscopic condensation/evaporation coefficients owing to the restricted molecular translational motion in the transition state.[15] The translational length ratio $\sqrt[3]{\nu_l/\nu_g}$ is an important factor to determine both the microscopic and macroscopic condensation/evaporation coefficients. The translational length ratio reveals that the nature of condensation/evaporation is directly related to the translational motion of the liquid and vapor molecules, and that, for a given pure liquid–vapor interface, the condensation/evaporation coefficient is an inherent property.

Table III lists the mean condensation/evaporation coefficients at different temperatures based on MD simulations. It is clear that the condensation/evaporation coefficient decreases with increasing temperature. A comparison between the MD results and the theoretical predictions of Eq. (3) is shown in Fig. 6. In our previous paper, the free volumes of liquid and vapor were assumed to be approximately equal to the specific volumes per mole of liquid and vapor molecules. This assumption is valid for an ideal state in which the actual volume

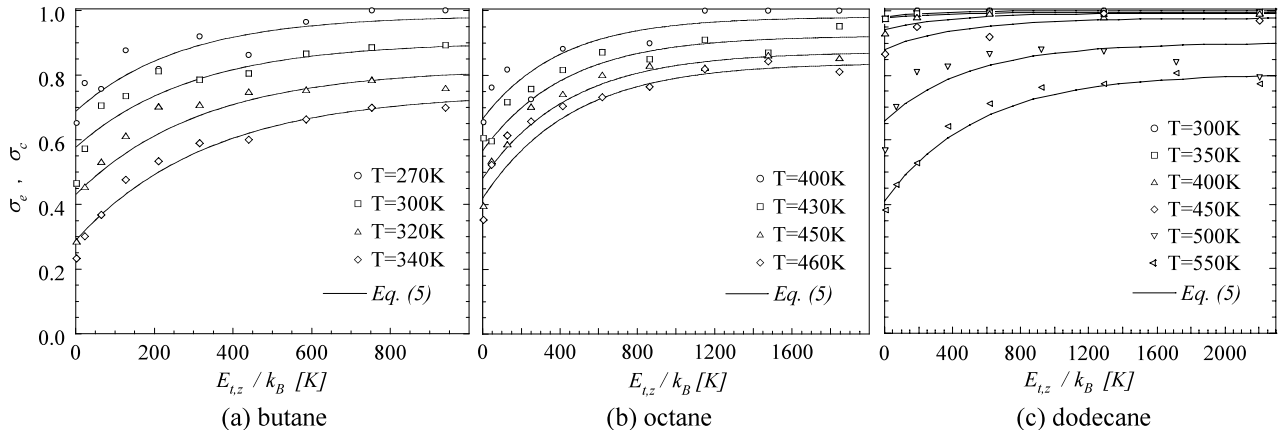

FIG. 5. Microscopic condensation/evaporation coefficients as a function of the normal component of molecular translation energy and temperature for (a) butane, (b) octane, and (c) dodecane.

TABLE III. Present MD simulation results of the condensation/evaporation coefficients and parameters in Eq. (5).

		Condensation/evaporation coefficient		
	T (K)	α	β	$\overline{\sigma}_e = \overline{\sigma}_c$
Butane	270	0.985	0.301	0.837
	300	0.903	0.361	0.740
	320	0.821	0.475	0.626
	340	0.746	0.612	0.518
Octane	400	0.981	0.321	0.824
	430	0.923	0.385	0.745
	450	0.873	0.448	0.677
	460	0.839	0.499	0.630
Dodecane	300	1.000	0.020	0.990
	350	0.995	0.017	0.986
	400	0.993	0.051	0.968
	450	0.977	0.099	0.929
	500	0.901	0.269	0.780
	550	0.805	0.489	0.608

of a mole of molecules can be neglected. However, for a real state, the actual molecular volume cannot be neglected; thus, the ratio of the cubic roots of the free volumes of liquid to vapor is smaller than that estimated using the specific volumes. As shown in Fig. 6(a), the present MD results, under the assumption that the free volumes equal the specific volumes, agree with the theoretical predictions of Eq. (3), but with a slight deviation. This deviation is reduced when the free volume is calculated as the volume difference between the specific volume and the molecular volume, as shown in Fig. 6(b). Here, the actual molecular volume v_m is assumed to be the van der Waals constant b, where $b = v_c/3$ and v_c is the specific volume per mole at the critical point. The deviation between the MD results and Eq. (3) could also be caused by errors in the density values, which could be a result of the applied potential model and the limited cutoff distance, and by the inaccuracy of the liquid–vapor interface position[19,24] or the distinct time of condensation/evaporation.[24] However, there is no noticeable difference among the results of butane, octane, and dodecane, which implies that the molecular chain length has little effect on the condensation/evaporation behavior.

D. Molecular orientation

The orientation of molecules can be studied using the orientation order parameter,

$$S = \frac{1}{2}\left\langle 3\sin^2\varphi - 1\right\rangle, \tag{8}$$

where φ is the angle between a vector that represents the molecular orientation and the unit vector parallel to the interface. Here, $\langle\cdots\rangle$ represents an ensemble average over all vectors connecting the neighboring carbon atoms of the backbone segments. The value of the order parameter is zero for a set of randomly oriented vectors (or perfectly ordered vectors of $\varphi \approx 35°$), unity for all vectors aligned perpendicularly to the interface, and −0.5 for all vectors aligned parallel to the interface. To characterize the molecular orientation, we use two different definitions for the ensemble average, as described below.

To represent the overall orientation of the simulation system, an ensemble average over all vectors within a specified slab in the z-direction was used. Figure 7 shows the orientation order parameter profile along the z-direction, S(z), in the vicinity of the interface for butane at 270 K and 340 K, octane at 400 K and 460 K, and dodecane at 300 K and 550 K. In all cases, the orientation is random in the bulk liquid ($z/L_z = 0.5$ is located at the center of the liquid film), whereas the chains show slight surface ordering at low temperatures. However, the ordering at the interface is not strong because the order parameter is small. Additionally, the surface ordering decreases with increasing temperature, and the orientation behavior at the interface for all examined molecules is similar to that reported for chain molecules, such as perfluorinated alkanes, fluorocarbons, semifluorinated alkanes, and hydrocarbon n-alkanes.[38–41] The observation that the condensation/evaporation coefficient is close to unity at low temperatures and decreases with increasing temperature implies that the effect of surface ordering on the condensation/evaporation coefficient is insignificant.

To represent the orientation of the backbone segments for each molecule, an ensemble average over all intermolecular vectors (three for butane, seven for octane, and eleven for dodecane) was used. The sample molecules passing through the interface were collected in the same way as those samples used for condensation, evaporation, and reflection at the interface. Figure 8 shows the probability density distributions

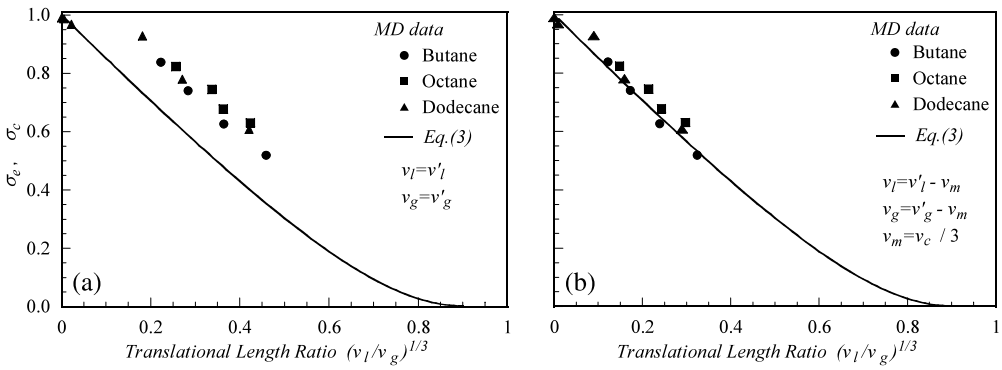

FIG. 6. Macroscopic condensation/evaporation coefficient as a function of translational length ratio.

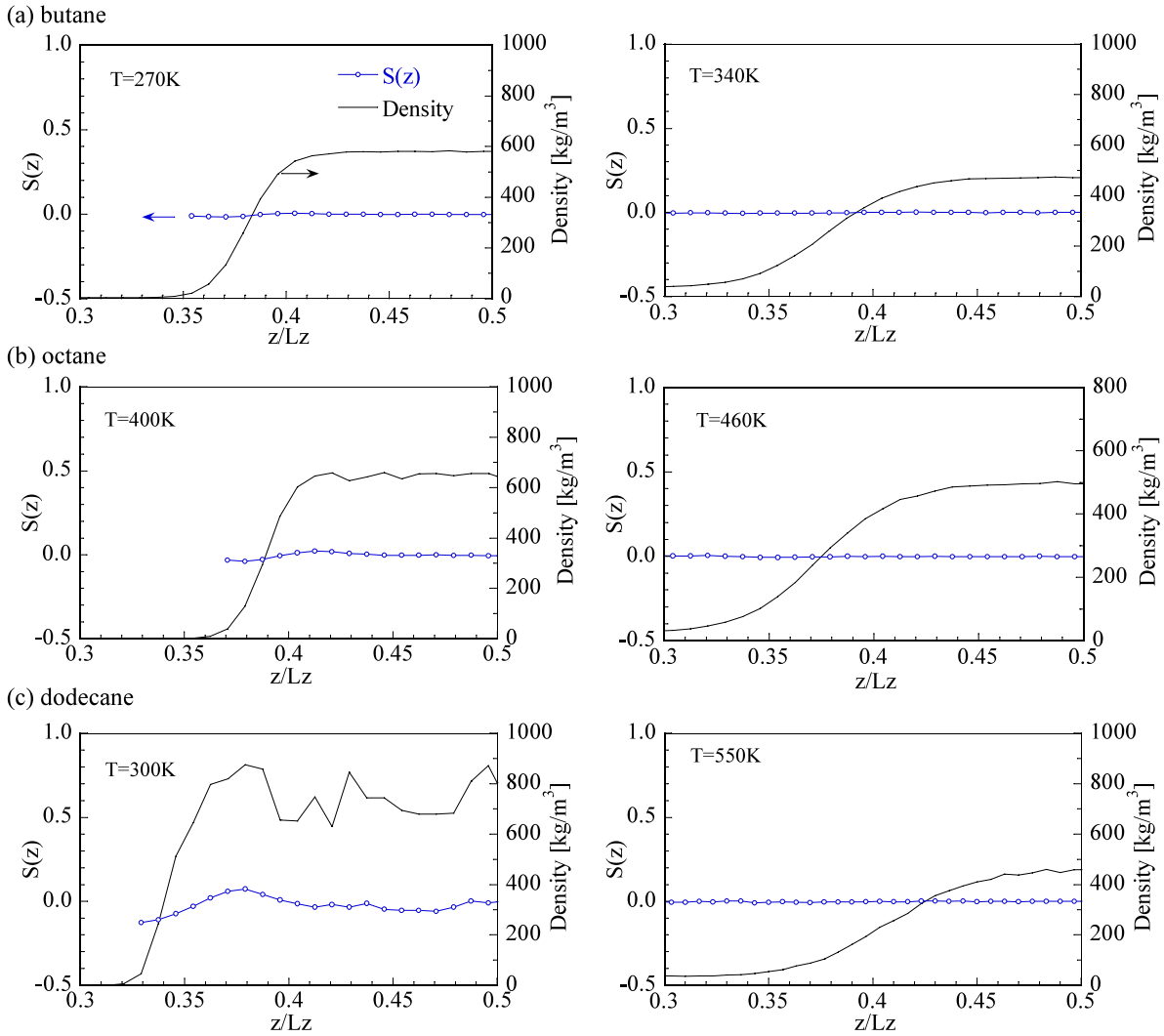

FIG. 7. Orientation order parameter profiles S(z) at the vicinity of the liquid–vapor interface.

of the orientation order parameter for all incoming/outgoing molecules as well as the condensed/evaporated molecules at different temperatures. It was observed that the probability density distribution of the orientation order parameter depended on the chain length, while no significant difference was observed between the probability density distribution of the orientation order parameters of incoming/outgoing and condensing/evaporating molecules. It should be noted that the

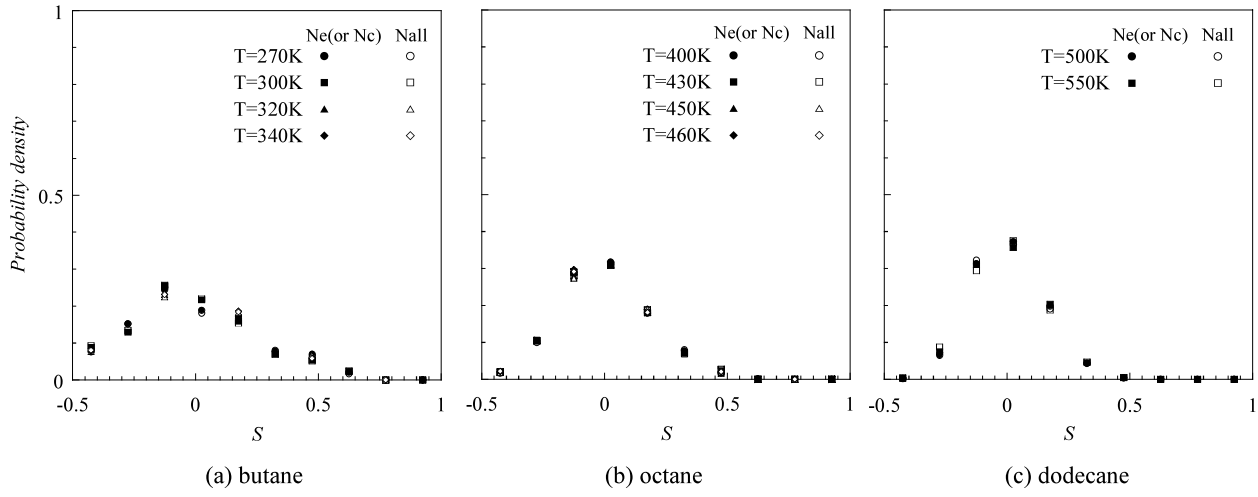

FIG. 8. Probability density distributions of the orientation order parameter S for the evaporated or condensed molecules (closed symbols) and all outgoing or incoming molecules (open symbols).

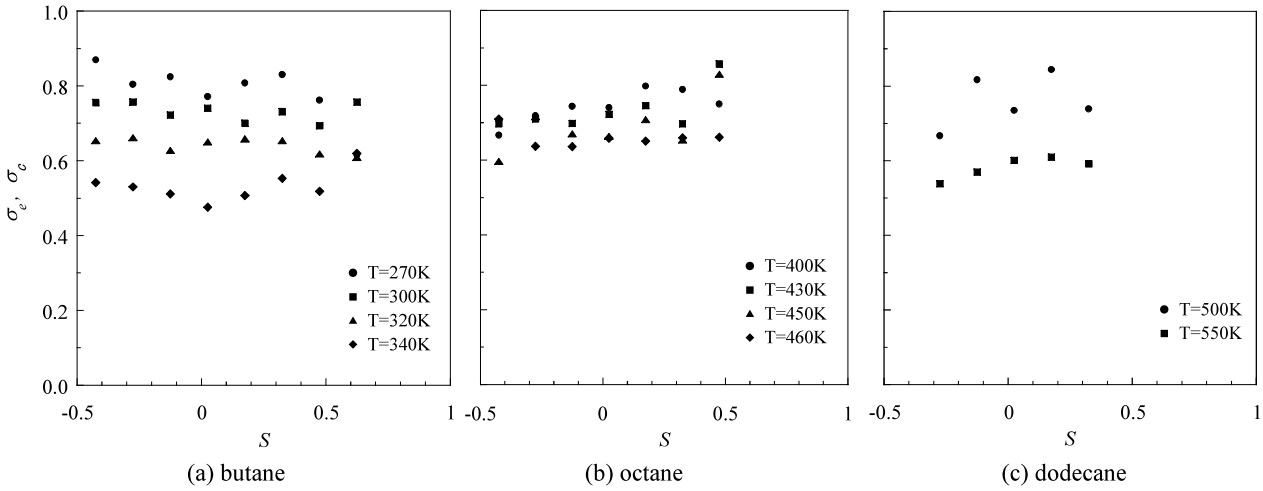

FIG. 9. Orientation order parameter and the condensation/evaporation coefficients for (a) butane, (b) octane, and (c) dodecane.

probability of the order parameter being S = −0.5 or S = 1 is almost zero; hence, the molecular orientation is neither normal nor parallel to the surface. Figure 9 summarizes the condensation/evaporation coefficients in relation to the molecular orientation and shows that, although there are fluctuations, the condensation/evaporation coefficients exhibit a tendency to be independent of the molecular orientation.

Based on the above results, we can conclude that the molecular orientation of the examined carbon chain molecule has no noticeable effect on the condensation/evaporation behavior. At the liquid–vapor interface, the amount of surface orientation of the chains depends on the temperature and on the chain length, while the molecular structure is unrelated to the condensation/evaporation coefficient. Consequently, the isotropic assumption related to the translation length ratio of liquid to vapor is appropriate, and Eq. (3) can be used to calculate the condensation/evaporation coefficient using this ratio, even for chain molecules.

IV. CONCLUSIONS

We performed MD simulations to investigate the condensation/evaporation coefficients of a group of carbon chain molecules: butane, octane, and dodecane. The obtained MD simulation data were consistent with the theoretical expression based on transition state theory, showing a dependence on the translational energy and the surface temperature similar to simple molecules like argon and water. A physical explanation is provided on the basis that the molecular orientation at the liquid–vapor interface is disordered when the surface temperature is sufficiently higher than the triple point and the molecular orientation has no significant effect on the molecular condensation/evaporation behavior.

Equation (3) enables us to predict the condensation/evaporation coefficients for most substances from their translational length ratio. Moreover, Eq. (3) provides a universal function if the validity of the isotropic assumption regarding the transition state of the liquid–vapor phase change is confirmed. Since the translational length ratio is the cubic root of the free volume ratio of liquid to vapor, the accuracy of the condensation/evaporation coefficients depends on the evaluation method of the free volume; however, it is difficult to obtain the free volume, particularly for long-chain molecules. For convenience, the free volume ratio can be approximated to the specific volume ratio, which could be obtained easily for most substances. This approximation results in larger free volume values (especially for liquid molecules) because the molecular volume is ignored; thus, the MD results deviate from Eq. (3). The deviation decreases when approximating the free volume as the difference between the specific volume and the molecular volume. However, the accuracy of the free volume values requires further investigation.

ACKNOWLEDGMENTS

This work is partially supported by the research supercomputing services by the Research Center for Computational Science and the Research Institute for Information Technology of Kyushu University.

[1]G. M. Pound, J. Phys. Chem. Ref. Data **1**, 135 (1972).
[2]M. Mozurkewich, Aerosol Sci. Technol. **5**, 223 (1986).
[3]I. W. Eames, N. J. Marr, and H. Sabir, Int. J. Heat Mass Transfer **40**, 2963 (1997).
[4]R. Marek and J. Straub, Int. J. Heat Mass Transfer **44**, 39 (2001).
[5]M. Matsumoto and Y. Kataoka, J. Chem. Phys. **90**, 2398 (1989).
[6]K. Yasuoka, M. Matsumoto, and Y. Kataoka, J. Chem. Phys. **101**, 7904 (1994).
[7]M. Matsumoto, K. Yasuoka, and Y. Kataoka, J. Chem. Phys. **101**, 7912 (1994).
[8]K. Yasuoka, M. Matsumoto, and Y. Kataoka, J. Mol. Liq. **65-66**, 329 (1995).
[9]M. Matsumoto, K. Yasuoka, and Y. Kataoka, Fluid Phase Equilib. **104**, 431 (1995).
[10]M. Matsumoto, Fluid Phase Equilib. **125**, 195 (1996).
[11]M. Matsumoto, Fluid Phase Equilib. **144**, 307 (1998).
[12]C. F. Clement, M. Kulmala, and T. Vesala, J. Aerosol Sci. **27**, 869 (1996).
[13]R. Meland, J. Chem. Phys. **117**, 7254 (2002).
[14]T. Tsuruta and G. Nagayama, J. Phys. Chem. B **108**, 1736 (2004).
[15]G. Nagayama and T. Tsuruta, J. Chem. Phys. **118**, 1392 (2003).
[16]T. Tsuruta, H. Tanaka, and T. Masuoka, Int. J. Heat Mass Transfer **42**, 4107 (1999).
[17]J. Vieceli, M. Roeselova, and D. J. Tobias, Chem. Phys. Lett. **393**, 249 (2004).
[18]A. Morita, M. Sugiyama, H. Kameda, S. Koda, and D. R. Hanson, J. Phys. Chem. B **108**, 9111 (2004).

[19]K. Gu, C. B. Watkins, and J. Koplik, Fluid Phase Equilib. **297**, 77 (2010).
[20]J. F. Xie, S. S. Sazhin, and B. Y. Cao, Phys. Fluids **23**, 112104 (2011).
[21]B. Y. Cao, J. F. Xie, and S. S. Sazhin, J. Chem. Phys. **134**, 164309 (2011).
[22]J. F. Xie, S. S. Sazhin, and B. Y. Cao, J. Therm. Sci. Technol. **7**, 288 (2012).
[23]H. Mizuguchi, G. Nagayama, and T. Tsuruta, Trans. Jpn. Soc. Mech. Eng., Ser. B **77**, 1826 (2011).
[24]G. Nagayama, M. Takematsu, and T. Tsuruta, Trans. Jpn. Soc. Mech. Eng. **79**, 2149 (2013).
[25]P. Louden, R. Schoenborn, and C. P. Lawrence, Fluid Phase Equilib. **349**, 83 (2013).
[26]A. Rosjorde, S. Kjelstrup, D. Bedeaux, and B. Hafskjold, J. Colloid Interface Sci. **240**, 355 (2001).
[27]R. Meland, A. Frezzotti, T. Ytrehus, and B. Hafskjold, Phys. Fluids **16**, 223 (2004).
[28]T. Ishiyama, T. Yano, and S. Fujikawa, Phys. Fluids **16**, 2899 (2004).
[29]T. Ishiyama, T. Yano, and S. Fujikawa, Phys. Fluids **16**, 4713 (2004).
[30]T. H. Yang and C. Pan, Int. J. Heat Mass Transfer **48**, 3516 (2005).
[31]S. F. Cheng, J. B. Lechman, S. J. Plimpton, and G. S. Grest, J. Chem. Phys. **134**, 224704 (2011).
[32]A. Lotfi, J. Vrabec, and J. Fischer, Int. J. Heat Mass Transfer **74**, 303 (2014).
[33]M. Zientara, D. Jakubczyk, M. Litniewski, and R. Holyst, J. Phys. Chem. C **117**, 1146 (2013).
[34]See http://www.gaussian.com/ for information about molecule structure modeling.
[35]See http://ambermd.org/ for information about the package of molecular simulation programs.
[36]J. Wang, R. M. Wolf, J. W. Caldwell, P. A. Kollmann, and D. A. Case, J. Comput. Chem. **25**, 1157 (2004).
[37]See http://www.nist.gov/ for Chemistry WebBook.
[38]K. C. Duffey, O. Shih, N. L. Wong, W. S. Drisdell, R. J. Saykally, and R. C. Cohen, Phys. Chem. Chem. Phys. **15**, 11634 (2013).
[39]M. Tsige and G. S. Grest, J. Phys. Chem. C **112**, 5029 (2008).
[40]A. Hariharan and J. G. Harris, J. Chem. Phys. **101**, 4156 (1994).
[41]H. K. Chilukoti, G. Kikugawa, and T. Ohara, Int. J. Heat Mass Transfer **59**, 144 (2013).